J Neurophysiol 106: 437–448, 2011.
First published May 4, 2011; doi:10.1152/jn.00010.2011.

Stability in a frontal plane model of balance requires coupled changes to postural configuration and neural feedback control

Jeffrey T. Bingham,[1] Julia T. Choi,[2] and Lena H. Ting[1,2]
[1]*Woodruff School of Mechanical Engineering, Georgia Institute of Technology, Atlanta; and* [2]*Wallace H. Coulter Department of Biomedical Engineering, Georgia Institute of Technology and Emory University, Atlanta, Georgia*

Submitted 5 January 2011; accepted in final form 2 May 2011

Bingham JT, Choi JT, Ting LH. Stability in a frontal plane model of balance requires coupled changes to postural configuration and neural feedback control. *J Neurophysiol* 106: 437–448, 2011. First published May 4, 2011; doi:10.1152/jn.00010.2011.—Postural stability depends on interactions between the musculoskeletal system and neural control mechanisms. We present a frontal plane model stabilized by delayed feedback to analyze the effects of altered stance width on postural responses to perturbations. We hypothesized that changing stance width alters the mechanical dynamics of the body and limits the range of delayed feedback gains that produce stable postural behaviors. Surprisingly, mechanical stability was found to decrease as stance width increased due to decreased effective inertia. Furthermore, due to sensorimotor delays and increased leverage of hip joint torque on center-of-mass motion, the magnitudes of the stabilizing delayed feedback gains decreased as stance width increased. Moreover, the ranges of the stable feedback gains were nonoverlapping across different stance widths such that using a single neural feedback control strategy at both narrow and wide stances could lead to instability. The set of stable feedback gains was further reduced by constraints on foot lift-off and perturbation magnitude. Simulations were fit to experimentally measured kinematics, and the identified feedback gains corroborated model predictions. In addition, analytical gain margin of the linearized system was found to predict step transitions without the need for simulation. In conclusion, this model offers a method to dissociate the complex interactions between postural configuration, delayed sensorimotor feedback, and nonlinear foot lift-off constraints. The model demonstrates that stability at wide stances can only be achieved if delayed neural feedback gains decrease. This model may be useful in explaining both expected and paradoxical changes in stance width in healthy and neurologically impaired individuals.

feedback model; frontal plan kinematics; perturbation response; posture and balance; sensorimotor

IF YOU ARE STANDING, do you feel more stable with your feet close together or spread apart? Changes in postural configuration affect the dynamics of the body and likely necessitate changes in neural control to perform a movement. Changes in stance width in a simple robotic model of standing balance control were found to be destabilizing without coordinated adjustments in physiologically inspired delayed feedback control gains for moderate perturbations (Scrivens et al. 2008). The nervous system likely selects specific postural configurations to reduce the neural demand for a task. For example, subjects have been observed to choose arm configurations that increase stability along directions of environmental instability (Trumbower et al. 2009). The selection of a postural configuration may also reduce energy expenditure or sensitivity to noise (Selen et al. 2009). Although this evidence demonstrates the importance of neuromechanical interactions in understanding motor control, little is known about the individual contributions and interplay between biomechanical and neural components that are required for stable posture and movement.

Consistent with our intuitions about standing balance control, wider stance widths are often considered to provide increased mechanical stability (Winter 1995), but little quantitative evidence exists to support these suppositions. The preferred stance width in healthy individuals is approximately equal to hip width (McIlroy and Maki 1997; Seidel et al. 1995). However, in uncertain conditions, like riding on a moving train, we often adopt a wider stance. In healthy subjects, muscle activation decreases in response to the same external perturbation when standing with wider stance, while the body's center-of-mass displacement stays roughly the same across different stance widths (Henry et al. 2001; Torres-Oviedo and Ting 2010). This has been suggested to be due to increased reliance on passive stability mechanisms and a reduction in neural control (Henry et al. 2001). However, these observations cannot be used to dissociate the contributions of biomechanical and neural systems to stability during these behaviors. Evidence from patients with neural deficits suggests that increasing stance width alone may not be stabilizing. Patients with Parkinson's disease who suffer from high postural instability exhibit deficits in appropriate scaling of postural feedback gains (Kim et al. 2009) and tend to choose a narrower stance, roughly one-half as wide as matched healthy controls (Horak et al. 2005). To better understand both healthy and neurologically impaired subjects, a frontal plane model with delayed feedback is necessary to quantify the neuromechanical interactions underlying stable balance control across postural configurations.

Physiological delays are significant during postural control and can limit the range of feedback gains that generate stability; however, the consequences for how balance is controlled in the frontal plane are not known. Active responses in muscles that restore the body center of mass occur at a latency of ~100 ms, and the resulting musculoskeletal forces are further delayed by 50 ms due to the time course associated with muscle force production and transmission (Horak and Macpherson 1996). As a result of this delay, the maximum magnitude of sensorimotor feedback gain is limited, with longer latencies reducing the set of feasible gains (Masani et al. 2008; Peterka 2009). Delayed feedback models of posture have been used to identify the complex stable boundaries of anterior-posterior balance (Masani et al. 2008; Mergner et

Address for reprint requests and other correspondence: L. H. Ting, 313 Ferst Drive NE, U.A. Whitaker Bldg. 3111, Atlanta, GA 30332-0535 (e-mail: lting@emory.edu).

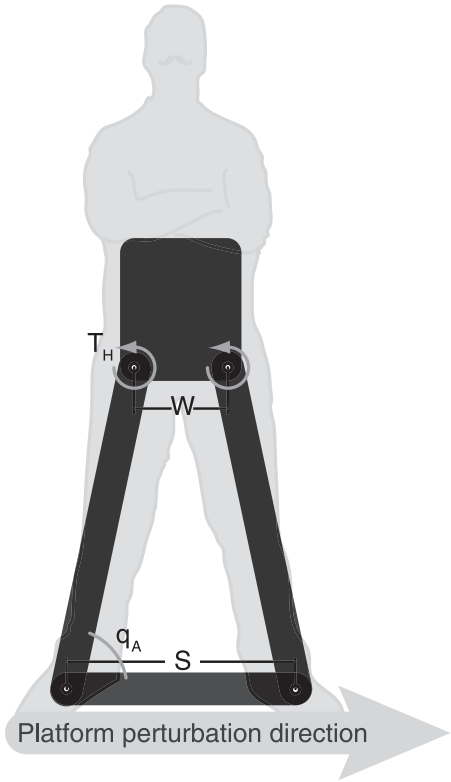

Fig. 1. Frontal plane model of human mediolateral balance control. Frontal plane motion of the body is modeled as a four-bar linkage. Two bars represent the legs, the third bar is the torso, and the fourth bar is the ground. Perturbations are applied as ground translations. Important parameters of the model are the hip width (W), stance width (S), hip torque (T_H), and ankle angle (q_A).

al. 2003; Milton et al. 2008; Peterka 2002; Van Der Kooij et al. 2001). Furthermore, delayed feedback models have been used to describe the entire time course of muscle activity during sagittal plane postural responses in both cats and humans (Lockhart and Ting 2007; Welch and Ting 2008). However, feedback control of frontal plane balance has received little attention and may be more dramatically influenced by postural configuration (Goodworth and Peterka 2010; Scrivens et al. 2008).

We hypothesized that changing stance width during standing balance control alters the neuromechanical interactions, necessitating appropriate adjustments of neural feedback gains to maintain stability. We performed analytical and computational analysis on a simple frontal plane model to examine how delayed feedback control of standing balance must change as a function of stance width. In our model, we examined the mechanical stability of the body alone and as stabilized by delayed feedback control. We also considered foot lift-off constraints and the effect of perturbation size on the robustness of stability during balance control. Our results showed that many different feedback gains produce stable behavior for each stance width. However, stable balance was not possible with a single feedback gain across all stance widths. This suggests that reduction of muscle activity in wide stance is not due to increased biomechanical stability in wide stance. Rather, increased sensitivity of body motion to joint torque production may necessitate that the nervous system appropriately tune feedback gains according to the biomechanical context.

METHODS

We developed a model of frontal plane balance to investigate the effects of postural configuration and delayed feedback control on stability to perturbations as stance width changed. We first quantified biomechanical properties and the stability of the model in the absence of feedback control as stance width changed. To investigate how postural configuration influenced the effect of feedback information during perturbations, we identified a relationship between hip angle and center-of-mass motion to a generalized coordinate (ankle angle). Next, the stability of the model under delayed feedback control was analyzed subject to different combinations of configuration, feedback gains, and delay. Furthermore, we determined how foot lift-off constraints and perturbation magnitude further reduced the feasible range of delayed feedback gains. Finally, we compared model predictions with recorded frontal plane motion in human experiments. Details about the model are provided in the Appendix and are summarized in the text.

Frontal Plane Model of Balance

To simulate and analyze frontal plane motion of an adult human, we modeled the body segments as a four-bar linkage and the neural control as delayed position and velocity feedback. The linkage consisted of four segments corresponding to the ground, two legs, and the torso connected by pin joints in a closed chain (Fig. 1). Inertial and geometric properties were based on average anthropometric data for an adult male with a height of 1.8 m and weight of 70 kg (Table 1) (Winter 2003). The leg segments were a lumped representation of the shank and thigh with a locked knee and pin joints for the ankle and hip. The torso segment included head, arms (folded across the chest), trunk, and pelvis and was attached to the leg segments by pin joints at the hips. The ground segment was considered immobile, and its length was used to specify the stance width of the model.

The equations of motion for the four-bar linkage were derived using a symbolic dynamics package (AutoLev 4.1; OnLine Dynamics) and matched those found in engineering texts (Norton 2001). The nonlinear equations of motion had one mechanical degree of freedom, which was specified by a generalized coordinate defined by the angle between the ground and the left leg, i.e., the ankle angle. Muscular force was modeled as a lumped term and applied with constant moment arms as torque about each hip joint. Perturbations to the model were included in the equations of motion as a time-varying acceleration to the inertial frame.

Hip torque was generated as delayed feedback with fixed gains on position and velocity. Feedback was dependent on either hip joint angle or center-of-mass horizontal excursion. Analysis of the model

Table 1. *Anthropometric data for four-bar linkage model of human standing*

Description	Symbol	Value	Unit
Nominal human mass	m_T	70	kg
Nominal human height	h_T	1.8	m
Leg mass	m_{leg}	$0.161 \cdot m_T$	kg
Leg length	L	$0.530 \cdot h_T$	m
Leg CoM with respect to ankle	L_{COM}	$0.293 \cdot h_T$	m
Leg inertia with respect to CoM	I_{leg}	$0.030 \cdot m_T(h_T)^2$	kg·m^2
Trunk mass	m_{trunk}	$0.678 \cdot m_T$	kg
Trunk CoM with respect to hip joint	H_{COM}	$0.108 \cdot h_T$	m
Trunk inertia with respect to CoM	I_{trunk}	$0.020 \cdot m_T(h_T)^2$	kg·m^2
Width between hip joints	W	$0.134 \cdot h_T$	m

CoM, center of mass.

was done using hip joint feedback unless stated otherwise. The delay was selected to be a single lumped value of 150 ms to account for neural transmission from sensation to actuation (100 ms) and mechanical actuation (50 ms) as observed from the automatic postural response (Horak and Macpherson 1996).

The perturbation applied to the four-bar linkage was applied as an inertial acceleration of the ground that matched platform translations from experimental ramp-and-hold protocols. The acceleration profile consisted of two Gaussian pulses with opposite directions, each 40 ms wide, spaced 500 ms apart, and having amplitudes ranging from 0.1 to 0.5 times earth gravity (g). This perturbation resulted in a zero starting velocity and a constant velocity movement phase, and finally ended at rest.

In addition, we performed numerical simulation of the equations of motion in Matlab. Integration was performed with the explicit trapezoidal rule with a step size of 1 ms and a total simulation time of 6 s. Initial conditions and state history were assumed to be zero. The perturbation was introduced as previously described. Center-of-mass trajectories and ground reaction forces were then recorded.

Biomechanical Stability Analysis

We identified stance width-dependent changes in the biomechanical properties of the model as quantified by the inertia, gravitational moment, sensitivity of the center-of-mass motion to joint torque, and the stability of the model, as defined by the eventual return of the model to an equilibrium position after a perturbation. The equilibrium position of the model was defined by the symmetrical configuration (Fig. 1) where all external forces were statically balanced, the center-of-mass was midway between the ankle joints, and the hip angles were equal. Inertia, gravitational moment, and joint torque were determined by linearizing the uncontrolled equations of motion with respect to the generalized coordinate and plotting them as functions of stance ratio (stance width divided by hip width, S/W). The anthropometric properties of an average adult male human were used for the plots (Table 1).

Inertia is a measure of an object's resistance to a change in motion and was used as an indicator of whether acceleration of the body would result in large motions (small inertia) or small motions (large inertia). Linearized inertia was calculated from the nonlinear equations of motion, resulting in a configuration-dependent term (see Appendix, *Eq. 7*). The linearized inertia was used to quantify the magnitude of center-of-mass motion from accelerations induced by perturbations and joint torques.

Although gravity is constant, it presents a destabilizing perturbation that is configuration dependent and is mathematically equivalent to a negative, or destabilizing, stiffness. A large magnitude of the linearized gravitational stiffness would result in a large destabilizing perturbation for a small deviation from the equilibrium configuration. The linearized gravitational stiffness was also represented as a configuration-dependent lumped parameter (see Appendix, *Eq. 8*).

The sensitivity of the joint torque quantified the efficiency of transmitting torque at the hip to motion of the center of mass. This relationship was calculated by employing the law of power continuity, which states that the product of torque and angular velocity must be conserved throughout a linkage (Norton 2001). The amplification or attenuation of the effective torque due to changes in stance width was used to determine the efficiency of that configuration. Effective torque on the center of mass due to torque applied at the hip joints was written as a configuration-dependent term for the entire four-bar linkage (see Appendix, *Eq. 9*).

To investigate differences between center of mass and joint angle as possible feedback variables, we calculated linear relations between hip angle, center-of-mass horizontal excursion, and the generalized coordinate (ankle angle). Ratios from the linearized equations of motion were calculated that transformed a small increment in either hip angle or center-of-mass horizontal excursion into an increment in the generalized coordinate. These ratios were plotted as functions of S/W using average anthropometric values (Table 1).

Delayed Feedback Stability Analysis

To determine the stability of delayed feedback on the biomechanical system, we compared the hip joint feedback gains across different delays, stance widths, and perturbations. The stability of the hip joint feedback gains was found by solving the nonlinear equations of motion for the critically stable boundaries. These boundaries were defined mathematically by the feedback gain values that resulted in solutions to the characteristic equation having zero real part. Behaviorally, this boundary divided gains resulting in falls (unstable) from those that returned the center of mass to the equilibrium position (stable). Since the characteristic equation for the delayed system resulted in an infinite number of solutions, numerical techniques were utilized to solve for a finite number of eigenvalues and to check the analytical stability boundaries using custom Matlab routines and the DDE-BIFTOOL delayed-differential equation toolbox (Engelborghs et al. 2002).

To quantify the relative stability between different stable feedback gain values, we performed a frequency domain analysis of the linearized equations of motion. The measures of gain margin and phase margin were used to identify robustness and system performance to perturbation magnitude. Gain margin is defined as the loop gain measured when the excitation frequency causes a $-180°$ phase difference between input and output. This was used to quantify the perturbation magnitude the model could withstand, where a large gain margin implied the model was stable against a large perturbation. Phase margin is defined as the phase difference from $-180°$ measured when the excitation frequency results in a loop gain of 1. Similarly, a large phase margin was inferred to mean the model was stable for a large perturbation.

To model physiological boundaries of stability, we used numerical simulations to identify hip joint feedback gains that produced feet-on-ground behavior. Simulations were performed in a gridwise manner across S/W of 0.5–2.0, all stable feedback gains, and perturbation magnitude of 0.1–0.5 g. The ground reaction forces were calculated for each simulation and used to determine if foot lift-off could occur. If ground reaction forces changed in sign during simulation, the associated parameters were classified as producing foot lift-off behavior. For each perturbation magnitude and stance width, the hip joint feedback gains producing feet-on-ground behavior were identified, and the boundary of these gains was plotted.

Experimental Comparisons

To compare simulated and experimental results, we collected body segment kinematics and ground reaction forces from healthy human subjects during platform perturbations. All protocols were approved by the Georgia Tech and Emory University Institutional Review Boards and conformed to the Declaration of Helsinki. Five subjects (3 male, 2 female, 20.6 ± 1.8 yr of age) were recruited. Subjects stood with arms crossed and their feet spaced at three fixed distances of 10, 19, and 32 cm. Each foot was located on an individual calibrated force plate (AMTI, Watertown, MA) that recorded all six reaction forces and moments. Subjects were instructed to stand upright and to maintain balance during perturbations, but they were not given information about time of perturbation onset. Perturbations were administered with a custom platform (Factory Automation Systems, Atlanta, GA) with position and acceleration of the platform recorded. At each stance width, subjects received 10 ramp-and-hold platform perturbations in the mediolateral direction with the platform moving to the subject's left. The perturbations had an overall movement distance of 12 cm, a plateau velocity of 35 cm/s, and a peak acceleration of 0.45 g. Subjects could not predict perturbation onsets because intertrial intervals were varied between 5 and 15 s.

Subject kinematics were captured with a custom 26-marker set that included head-arms-trunk, thigh, shank, and foot segments with the use of a motion capture system (Vicon, Oxford, UK) utilizing 8

cameras. Motion capture was sampled at 120 Hz and platform kinematics at 1,080 Hz. Platform kinematics were low-pass filtered at 30 Hz (third-order, zero-lag, Butterworth filter) and combined with motion capture kinematics to produce relative position, velocity, and acceleration of the markers with respect to the platform. The relative motion of the markers and a proportional model of human mass were used to calculate center-of-mass position, velocity, and acceleration for each subject (Winter 2003).

Simulated center-of-mass position was fit to experimental data through optimization of the feedback gains for the nonlinear equations of motion. Fits were calculated for two feedback rules, one using hip angle and the other center-of-mass excursion. Each experimental trial was fit using the subject's measured mass, height, stance width, and perturbation acceleration profile. For a given subject and stance width, model parameters were fixed and only feedback gain values were allowed to vary. This resulted in a total of 300 fits: 2 feedback rules by 10 perturbations by 3 stance widths by 5 subjects. Optimization to solve for the feedback gains utilized a cost function defined by the difference between simulated and experimental center-of-mass trajectories with penalties on absolute (weight of 1) and sum-squared error (weight of 10).

RESULTS

Mechanical Stability Decreased With Increasing Stance Width

Inertia decreased with increasing stance width. The linearized inertia about the equilibrium configuration was found to decrease as stance width increased within the physiological range (Fig. 2*A*). The combined inertia of the body and legs was configuration dependent, changing with stance width and joint angle. Changes to stance width had the most affect on the apparent inertia of the body segment. Increasing stance width resulted in decreased inertia. Therefore, the same amount of applied torque produced at wide stance resulted in greater center-of-mass motion than when applied at narrow stance.

Gravitational stiffness remained constant with changing stance width. The destabilizing effect of gravity remained nearly constant across the physiological range of stance (Fig. 2*B*). In general, the gravitational stiffness was found to have a minimum near the stance ratio of 1 and increased to a maximum as stance width approached the singular configuration. The destabilizing effect of gravity therefore remained nearly constant for physiological stance ratios of 0.8–2.0.

Hip torque was more effective at wider stance. For constant torque at the hip, the effective torque on the center of mass increased as stance width increased. The amplification of the hip joint torque was found to quadratically increase with stance width. As stance width increased, the same input torque produced a greater total torque on the motion of the four-bar linkage (Fig. 2*C*). In other words, torque applied at the hip had more leverage on the center of mass at wider stances.

Model without delayed feedback was unstable across stance widths. The four-bar linkage without torque feedback was found to be unstable for all physiological stance widths. Stability decreased as stance width increased due to decreasing inertia while the destabilizing gravitational stiffness remained constant. To stabilize the mechanical system with delayed feedback, both position and velocity were required. Position feedback was required to counteract destabilizing gravitational stiffness, and velocity feedback was required to produce a damped response.

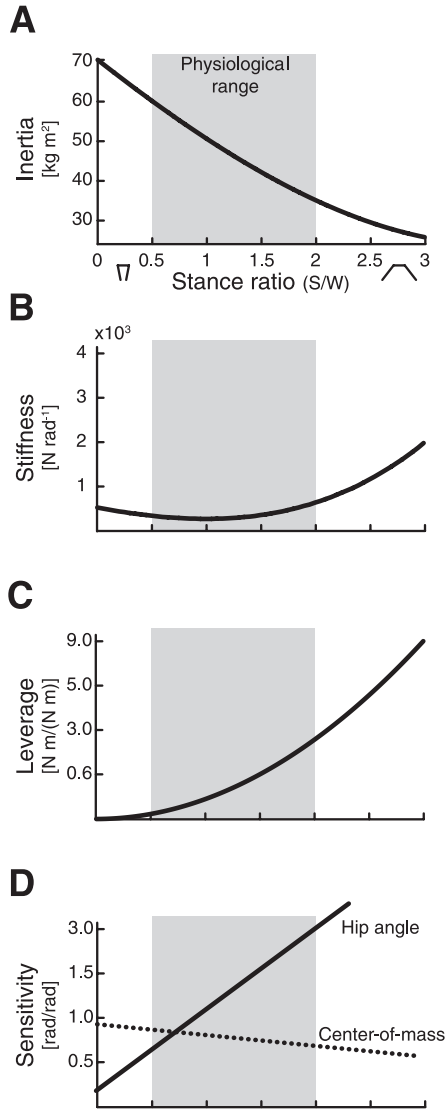

Fig. 2. Changes in biomechanical properties of the body as stance width increases. For a nominal human (70 kg, 1.8 m), as stance width increased, inertia decreased (*A*), gravitational "stiffness" stayed roughly the same (*B*), hip torque leverage increased (*C*), and hip angle sensitivity to ankle angle changes increased (*D*; center-of-mass sensitivity decreased slightly), all of which resulted in decreased biomechanical stability. Shaded regions mark physiological stance ratios (*S*/*W*).

Center of mass and joint angle feedback scale linearly across stance widths. The effect of a small change in the generalized coordinate (ankle angle) on the hip angle or center-of-mass excursion changed proportionally with different stance widths (Fig. 2*D*). The hip angle became more sensitive to changes in ankle angle as stance width increased. Conversely, the center-of-mass excursion decreased in sensitivity to changes in ankle angle with increasing stance width. Center-of-mass excursion was more sensitive to changes in ankle angle than hip angle for $S/W < 0.8$, and hip angle was more sensitive to changes in ankle angle at wider stances. Furthermore, sensitivity to changes in ankle angle varied much less for center-of-mass excursion compared with hip angle over the physiological range. A small perturbation to the overall body angle resulted in larger excursion of the hip angle at wide stances. The linear relationships to the generalized coordinate

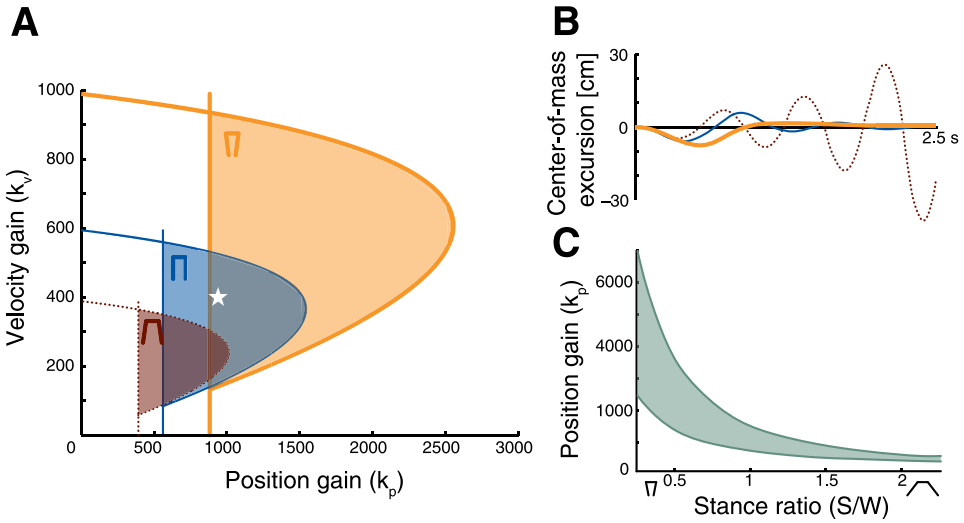

Fig. 3. Regions of stable feedback gains across stance widths demonstrate that a fixed set of gains was not stable across different stance widths. *A*: shaded areas represent stable position and velocity feedback gain values for a nominal human (70 kg, 1.8 m) with stance ratios of 0.8 (dotted line), 1.0 (thin line), and 1.2 (thick line). *B*: center-of-mass trajectories resulting from a 0.4-*g* perturbation for each stance ratio using the same gain value as in *A*, marked as a white star in gain space. *C*: stable position feedback gain (k_p) values across all physiological stance widths.

predicted the nonlinear feedback gains on center-of-mass excursion from hip joint angle feedback gains very closely.

Stable Feedback Gain Boundaries Decreased With Increasing Stance Width

Stable delayed feedback gains have upper and lower bounds. The stable limits for the delayed feedback gains produced D-shaped boundaries associated with functional instabilities (Fig. 3*A*). The boundaries were determined as a parametric solution to the characteristic equation (Appendix, *Eq. 12*). The left-hand boundary (Appendix, *Eq. 13*) represented a lower limit on delayed position feedback gain, k_p. The functional consequence of this limit corresponded to the delayed position feedback gain (k_p) being unable to counteract the destabilizing gravitational stiffness. The right-hand boundary (Appendix, *Eq. 14*) restricted both position and velocity feedback gains. This upper boundary was a consequence of the feedback delay and functionally represented instability due to overcorrection. Finally, an upper limit on the length of delay was found, 429 ms for an average human at preferred stance, for which there were no feedback gain values that were stable (Appendix, *Eq. 15*).

Stable gain space decreased with increasing stance width. The set of stable delayed position and velocity hip joint feedback gains was found to decrease as stance width increased (Fig. 3*A*). The maximum and minimum values of stable feedback gain were found to decrease as stance width increased. Specifically, narrow stance width ($S/W = 0.8$) was found to have 98% more gain space area than the wide stance width ($S/W = 2.0$). High gain values that were stable for narrow stance were unstable for wide stance. Stable gain regions did not completely overlap for different stance widths. However, even when overlap did occur, the simulated center-of-mass trajectories for the same gain across stance widths varied considerably (Fig. 3*B*). Similar results were found when center-of-mass excursion feedback was used; however, more overlap was observed in the stable gain regions across stance widths.

Ground Contact Reduced Set of Stable Feedback Gains

Ground contact constraint produced more physiological center-of-mass trajectories. Center-of-mass trajectories associated with hip joint feedback gains limited by the feet-on-ground condition matched more closely with experimentally observed trajectories. High stable feedback gains produced center-of-mass trajectories that were highly oscillatory in the model (Fig. 4). These did not match experimental observations of human motion that show near critically damped center-of-mass trajectories when subjected to a platform perturbation. Limiting stable feedback gains to those that produced

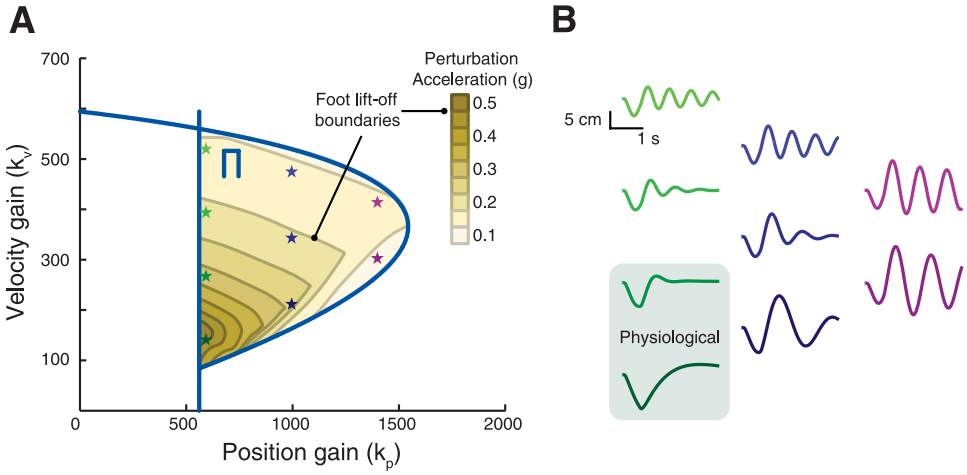

Fig. 4. Boundaries on physiological feedback gains due to foot lift-off criterion and damped center-of-mass dynamics for a nominal human (70 kg, 1.8m) with a stance ratio of 1.0. *A*: the thick outer line is the stability boundary without considering foot lift-off. The thin lines and shaded areas correspond to the boundaries for foot lift-off at different perturbation magnitudes. k_v, velocity feedback gain. *B*: center-of-mass trajectories for 0.4-*g* perturbation. Each trajectory corresponds to a gain pair marked by a colored star in *A*. Gains outside of the stability region due to foot lift-off produce nonphysiological, oscillatory motion of the center of mass, which requires the feet to pull up on the ground. Physiological trajectories shown in the gray-shaded region are close to critically damped and do not violate foot lift-off constraints.

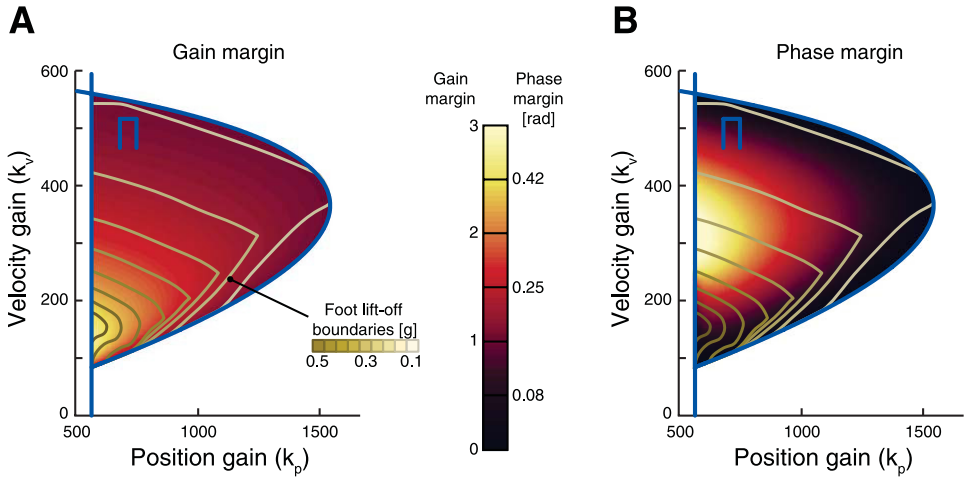

Fig. 5. Comparison of simulated stepping boundaries and analytical measures of relative stability. For a nominal human (70 kg, 1.8m) with a stance ratio of 1.0, thick outer lines represent stability boundaries and thin lines delineate nonstepping boundaries for different perturbations derived from simulations (see Fig. 4). Shaded gradient represents the magnitude of the analytical measures gain margin (*A*) and phase margin (*B*).

feet-on-ground behavior resulted in more physiological looking trajectories and removed highly oscillatory center-of-mass responses.

Stable gain space decreased as perturbation magnitude increased. Restricting stable hip joint feedback gains to those that produced simulations with feet-on-ground behavior when the model was subjected to a finite perturbation resulted in a reduction in the stable boundaries. Infinitesimally small perturbations resulted in feet-on-ground behavior for all feedback gain values determined from the analytical stable boundaries. However, as perturbation acceleration magnitude increased, the set of stable gains associated with feet-on-ground behavior was reduced (Fig. 4*A*). The gain space area of feet-on-ground behavior for a perturbation acceleration of 0.45 *g* and S/W = 1.0 was reduced by 96%.

Gain margin predicted simulated foot lift-off threshold. Similar foot lift-off thresholds were predicted from full nonlinear simulations as well as from the gain margin of the linearized system (Fig. 5*A*). From simulations, the right-hand stability boundary associated with delayed feedback and feet-on-ground behavior decreased in size as perturbation magnitude increased, whereas the left-hand boundary remained constant. As perturbation magnitude increased, this boundary decreased until no feedback gains were stable. The analytical measure of gain margin was found to increase as feedback gain decreased to the lower limits of position and velocity (Fig. 5*A*). A gain margin greater than six times the perturbation magnitude was capable of predicting stable feet-on-ground responses. The phase margin increased as position feedback decreased and velocity feedback was near the middle of its range (Fig. 5*B*). Gain and phase margin were found to be identical for both hip joint and center-of-mass excursion feedback.

Experimental feedback gain decreased as stance width increased. The full nonlinear simulated center-of-mass trajectories fit using hip feedback gains matched the experimental trajectories with an average root mean square error of 8.00 ± 2.82 mm (r^2 = 0.97 ± 0.02) across all subjects and trials (Fig. 6). The position and velocity feedback gains necessary to fit the center-of-mass trajectories were found to both decrease as stance width increased (Fig. 7, *A* and *B*). The fits using center-of-mass excursion feedback resulted in nearly identical fits to those calculated using hip joint feedback, and these gains were related closely by a fixed configuration-dependent ratio. Feedback gains were found to scale proportionally together with stance width at a ratio where position gain was ~3.6 times

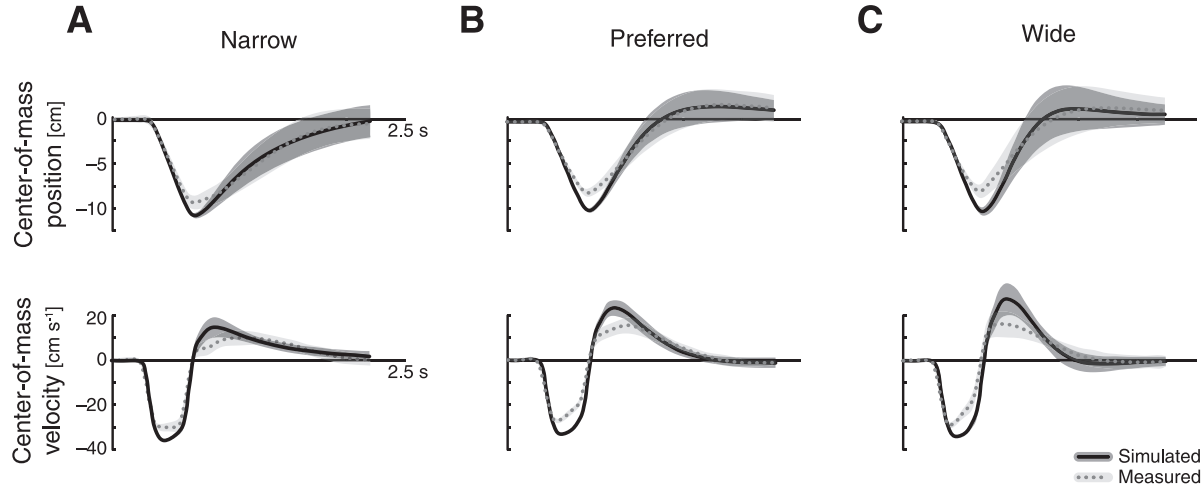

Fig. 6. Comparison of model trajectories fit to experimentally measured center-of-mass kinematics with respect to subjects' feet across stance widths. Lines represent average behavior across all subject trials, and shaded regions indicate the standard deviation. Solid lines represent simulation and dotted lines are experiments. Center-of-mass kinematics are similar in shape and maximum excursion across narrow (*A*; stance width = 10 cm), preferred (*B*; 19 cm), and wide stance (*C*; 32 cm).

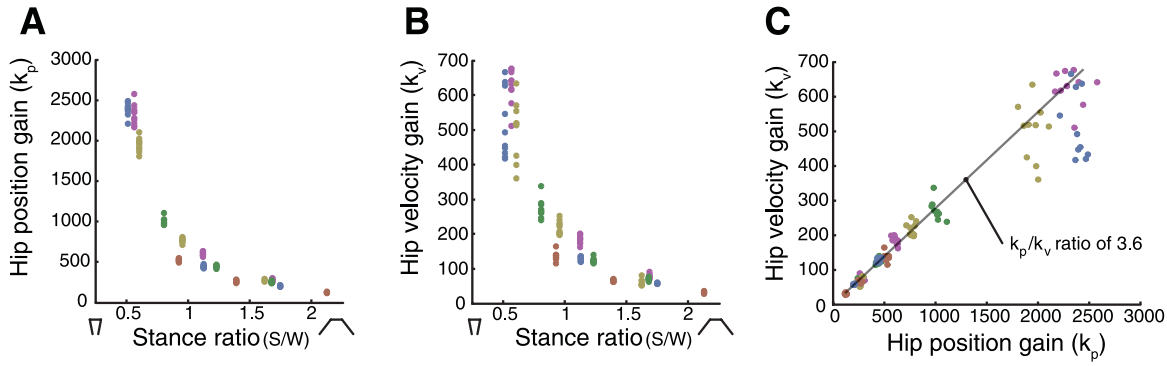

Fig. 7. Changes in subject feedback gains with stance width. Trial-by-trial variation in the position and velocity feedback gains of the model matched the measured center-of-mass trajectories across subjects. Feedback gains for position (*A*) and velocity (*B*) were similar across subjects, and variability decreased as stance width increased. *C*: the ratio of position to velocity feedback gain (k_p/k_v = 3.6) was consistent across subjects and stance widths.

velocity gain (see slope of line in Fig. 7*C*). Finally, the fitted feedback gains were found to have a gain margin larger than 1.5 (Fig. 8).

DISCUSSION

The seemingly simple act of increasing one's stance width requires that the nervous system appropriately alter delayed sensorimotor feedback gains due to the reduced torque required for stability at wider stance widths. Contrary to intuition, biomechanical stability decreases at wider stances due to the reduction in rotational inertia, while the destabilizing gravitational moment remains nearly constant. Without neuromuscular involvement, a wide stance is less stable than a narrow stance. The changes in the biomechanical properties of the body result in increased leverage and sensitivity of center-of-mass motion to changes in hip torque at wide stance. Maintaining the same center-of-mass motion in response to perturbations requires less hip torque at wide stance than at narrow stance. This prediction is consistent with observations that muscle activity from postural responses decreases with increasing stance width (Henry et al. 2001; Torres-Oviedo and Ting 2010). However, to achieve appropriate levels of stabilizing torque with delayed sensorimotor feedback, a decrease in gain is required as stance width increases. Therefore, feedback gains that are stable for a narrow stance width are unstable for a wide stance width (Fig. 3*A*). Thus, to maintain postural stability, the nervous system must rapidly adjust the magnitude of feedback gains appropriate for a selected postural configuration.

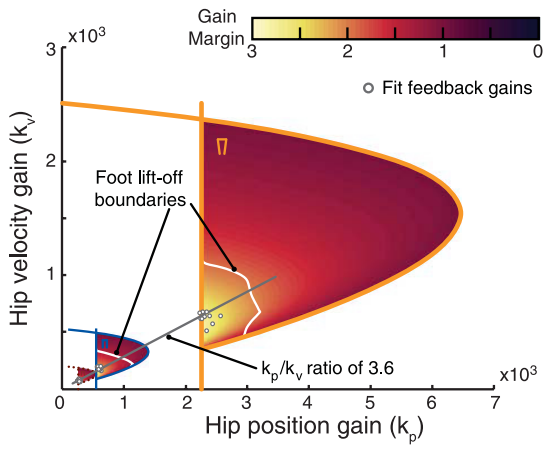

Fig. 8. Subject feedback gains overlaid on simulated stepping boundaries and gain margin. For a representative subject, the stability boundaries for narrow (thick line), preferred (thin line), and wide stance (dotted) are plotted with a gradient representing gain margin. The simulated foot lift-off boundary (white line) closely matched a lower bound on gain margin of 1.85. The white circles show the location of fitted feedback gains that lie within the stable boundaries.

Implications of Delayed Feedback, Stance Width, and Foot Lift-Off for Balance Control

Our model demonstrates that neural strategies for human postural control are constrained by physiological delays associated with the transmission of sensory and motor signals. Neuromechanical delays in healthy humans are relatively long, typically 150 ms for postural responses, which constrains the rapidity that neural feedback systems can affect body dynamics (Horak and Macpherson 1996). Delays result in upper bounds for feedback gains, since large gain magnitudes lead to instability (Stepan and Kollar 2000). Furthermore, as delays increase, the upper boundary and the set of stable feedback gains decreases (Masani et al. 2008; Peterka 2009; Scrivens et al. 2008; Sieber and Krauskopf 2004). The inclusion of delay in postural control models is thus necessary to appropriately predict the set of stable feedback gains for standing balance control (Masani et al. 2008; Mergner 2010; Peterka 2002; Van Der Kooij et al. 2001). In contrast, feedback models that omit physiological time delays (Kuo 1995; Park et al. 2004) would not identify the upper limits for feedback gains. The lack of an upper limit on allowable feedback gains could lead to the incorrect conclusion that a single set of gains would be sufficient for stability across different stance widths. Furthermore, H. S. Black's original concept of high-gain negative feedback may produce the unintended consequence that the control completely masks the underlying system dynamics (Black 1934). In contrast, biological systems tend to leverage the intrinsic biomechanical characteristics suitable for a desired behavior. Evidence of the importance of biomechanics in neural control is exemplified by passive dynamic walkers (McGeer 1990), resonance of feeding apparatus in aplysia (Ye et al. 2006), and multileg interaction in cockroaches running over rough terrain (Sponberg and Full 2008). Neglecting neural delay allows the application of high-gain feedback that is likely nonphysiological and may result in incorrect interpretations of closed-loop stability.

The set of feasible feedback gains are further constrained by the functional limits of foot lift-off. Utilizing a foot lift-off

criterion is important when identifying functional limits of stability. Many studies utilize an inverted pendulum to model postural control, because the-second order dynamics and gravitational instability capture the characteristics of observed center-of-mass motion (Lockhart and Ting 2007; Loram and Lakie 2002; Masani et al. 2008; Mergner 2010; Pai and Patton 1997; Peterka 2002; Winter et al. 1998). However, the simplicity of the inverted pendulum lacks straightforward methods for implementing realistic ground contact and determining the effects of configuration. Pendulum models alone may overestimate stability boundaries for a specific perturbation magnitude. Pai and Patton have addressed foot lift-off in sagittal plane models by imposing limitations on the amount of allowable torque at the base joint (Pai and Patton 1997; Pai et al. 2000). Foot lift-off in our four-bar linkage model utilizes the dynamics of the body and the nonlinear ground contact force, regardless of a subject's strength. Use of the four-bar linkage model may allow decoupling of muscle strength and skeletal dynamics effects for both sagittal and frontal plane studies. The four-bar linkage model could be readily adapted to sagittal plane analyses by setting the hip and stance width to the length of the foot.

Foot lift-off for a specified perturbation to the model can be estimated by an analytical measure of relative stability, gain margin. Relative stability allows for comparing stability under different conditions, which has been accomplished with numerical methods in previous research (Patton et al. 2000). Calculation of the gain margin does not require computationally costly simulations to quantify relative stability. Gain margin is a distance from the critically stable gain. For symmetric initial conditions, the gain margin for a set of feedback gains matches favorably with the stepping boundaries found through forward simulations of the four-bar linkage. Feedback gains with a higher gain margin can withstand larger perturbations. Feedback gains with common gain margin across stance widths lie on a line (Fig. 8). This suggests that position and velocity feedback gains can be scaled by a single parameter as stance width changes to maintain similar body dynamics. This may be a general principle of neural control for balance, since sagittal plane models also show proportional scaling of position and velocity feedback gains due to sensory reweighting (Peterka 2002). Furthermore, feedback gains fit to experimental data show that, despite changes in feedback gain magnitudes, individuals utilize feedback gains with a common gain margin across stance widths. Common gain margin across stance widths suggests neural feedback control is modulated to maintain a consistent level of stability, which may explain the consistency of center-of-mass trajectories across stance widths (Henry et al. 2001).

Modeling Assumptions and Limitations

The relative stability of feedback gains would increase with the addition of passive, nondelayed stiffness and damping but would not alter the primary result that delayed feedback gains must decrease as stance width increases. Without explicit intrinsic stiffness elements, our model is unable to identify stability conferred by muscle cocontraction when fit to experimental data (Franklin et al. 2003). Since nondelayed stiffness and damping produce a stabilizing effect (Hogan 1985), our model may result in a conservative estimate of delayed feedback gains. However, the relative contribution of nondelayed components to the stability of standing balance is likely small. Seminal work on ankle stiffness in seated subjects performing dorsi-plantar flexion reported values of 1.75 N·m/deg (100 N·m/rad) during passive behavior and up to 17.5 N·m/deg (1,000 N·m/rad) during active behavior (Weiss et al. 1988). The order of magnitude difference between passive and active stiffness has also been reported in postural tasks. Specifically, sagittal plane models of postural control have demonstrated that nondelayed feedback is 10 times smaller than delayed feedback during standing: 1.6 N·m/deg (92 N·m/rad) vs. 16.9 N·m/deg (968 N·m/rad), respectively (Loram and Lakie 2002; Peterka 2002). Adding physiological quantities of nondelayed stiffness and damping to our model only slightly increased the set of possible stable delayed feedback gains (Fig. 9*A*, lightest shaded area). Moreover, increasing nondelayed stiffness and damping 10-fold greater than physiological amounts still resulted in the sets of stable delayed feedback gains decreasing as stance width increased (Fig. 9*B*). Therefore, the addition of nondelayed elements does not alter the fundamental finding that delayed feedback gain must decrease as stance width increases, although passive elements may relax the amount of delayed feedback modulation required for stability (Ting et al. 2009). Furthermore, the inclusion of nondelayed feedback adds redundancy in the fitting of kinematic trajectories. When two delayed feedback gains were fit to match experimental center-of-mass trajectories, only a single solution was found. However, multiple, divergent solutions were found to produce equivalent center-of-mass trajectories when nondelayed feedback components were added (Fig. 9*C*). Thus it is not possible to distinguish the delayed and nondelayed stiffness components using our current methodologies. Muscle activity or independent measures of nondelayed stiffness and damping may be required to quantify these separate contributions. Nondelayed stiffness and damping are likely important factors to consider when analyzing pathological populations where muscle tone and muscle cocontraction are increased (Dietz and Sinkjaer 2007), which may emphasize the role of nondelayed feedback and reduce the contribution of delayed feedback for maintaining stability (Bunderson et al. 2008).

The single-degree of freedom nature of the four-bar linkage model leads to the result that torque applied at either of the ankles or hips can be equivalently represented as a torque at the hip. Therefore, the actions of the modeled hip torque could be equally achieved by a distribution of torques at the hip and ankle joints. Our model demonstrates that frontal plane inertia decreases as stance width increases, requiring that the magnitude of torque applied at any joint must also decrease to produce the same center-of-mass motion (Fig. 9*A*). Accordingly, activity in muscles producing torque at the hip and ankle is observed to scale with stance width in response to mediolateral perturbations (Henry 2001; Torres 2010). It is likely that a large proportion of torque is produced at the hip, since frontal plane peak hip torque (90 N·m) (Boling et al. 2009; Cuthbert and Goodheart 2007) is significantly greater than peak ankle torque (25 N·m) (Kaminski et al. 1999; Konradsen et al. 2005). Although peak torque is not necessarily representative of the proportion of torque produced at each joint for standing balance in sagittal perturbations (Kuo and Zajac 1993), hip torque is further favored in frontal plane balance control because

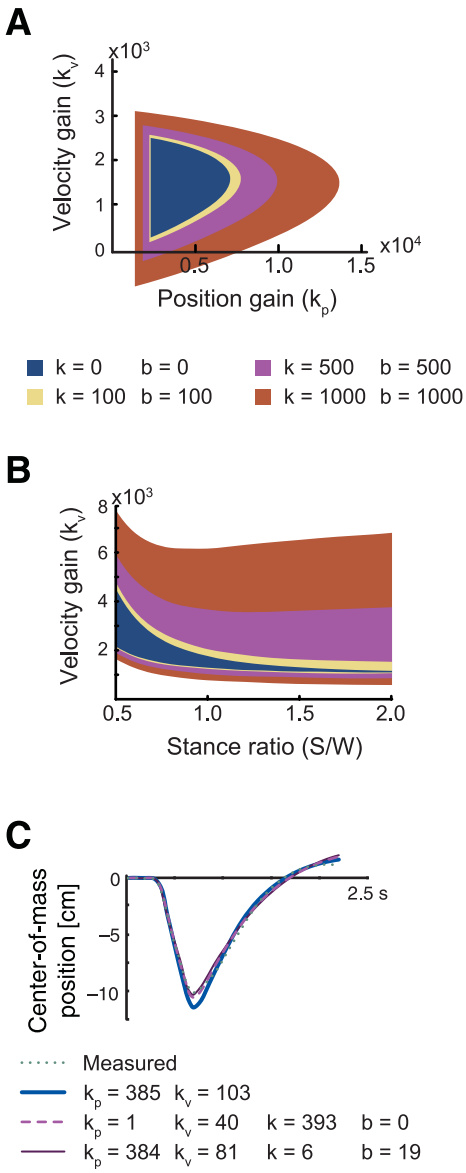

Fig. 9. Effect of nondelayed position and velocity feedback on stable sets of delayed feedback for a nominal human (70 kg, 1.8 m) with a stance ratio of 1.0. *A*: assuming physiological levels of nondelayed feedback (passive stiffness $k = 100$, damping $b = 100$) showed only slight increase in the allowable set of stable nondelayed feedback gains. *B*: large values of nondelayed feedback ($k = 500$, $b = 500$) resulted in decreased nondelayed feedback gain as stance width increased. *C*: if nondelayed feedback was used, multiple combinations of feedback gains (dashed and thin lines) reconstructed experimental kinematics (dotted line), whereas only 1 delayed gain pair (thick line) reproduced the trajectory.

leverage effects scale hip torque proportionally with stance width but do not scale ankle torque.

Our model accounts for a majority of the center-of-mass kinematics and may be improved by including additional degrees of freedom. When position and velocity feedback gains are adjusted, center-of-mass kinematics from nonlinear simulations match experimental observations with only slight overshoot of the maximum center-of-mass excursion (Fig. 6). This overshoot is more pronounced in wider stances, which may be due to an inability of the model to predict correct phasing between upper and lower body movement (Goodworth and Peterka 2010). These deviations in center-of-mass kinematics are small, and the model corroborates experimental observations of peak center-of-mass excursion remaining constant across stance widths (Henry et al. 2001). Previous modeling studies suggest that feedback control of human muscle activity may rely on an estimate of body center-of-mass motion, rather than local joint feedback (Welch and Ting 2008, 2009). This is consistent with neurophysiological evidence of global variables being encoded by the nervous system (Bosco and Poppele 1997). Remarkably, center-of-mass kinematics reproduced with either center-of-mass or joint feedback control were similar, even though these two feedback signals are not linearly related. The similarity in kinematic output precludes using system identification to distinguish between these strategies in the four-bar linkage model. We predict that a model with flexible knees and upper body would allow decoupling of the ankle and hip joints and potentially reveal differences in stability between center-of-mass and joint feedback control.

Model-Based Interpretation of Stance Width Adaptation

Despite the relative simplicity of our model, it provides new insight into the interdependence between neural and biomechanical stability during balance control. The healthy nervous system may exploit different combinations of feedback gain and posture configurations to flexibly achieve balance. Choosing a wider stance width necessitates reduced torque and may be advantageous when muscle torque generation is a limiting factor. As a result of increased leverage, wide stance may reduce the torque requirement during a perturbation response. However, the benefits of wide stance are countered by a reduction in maneuverability and an increase in static metabolic cost, which suggests why healthy individuals only select wide stance in unstable conditions. Furthermore, our model suggests that the increase in sensorimotor delay associated with aging (Woollacott et al. 1988) should result in decreased feedback gains (Allum et al. 2002) and smaller feasible feedback gains for maintaining stability at wide stances. Another possible compensation to increased delay may be to decrease stance width, which has been observed in elderly populations (McIlroy and Maki 1997; Swanenburg et al. 2010).

Changes in postural stability during and following pregnancy may be explained by our model if long-term adaptation of neural feedback to changes is slow compared with biomechanical changes in postural configuration. During pregnancy, stance width increases gradually and frontal plane sway remains consistent. However, shortly after delivery, preferred stance width returns to prepregnancy width and frontal plane sway increases (Jang et al. 2008). We hypothesize that the set point for sensorimotor feedback gains adapt slowly to the increasing stance width over the course of pregnancy. The decrease in stability postpartum may be due to using low feedback gains appropriate for wide stance at the preferred stance width, generating a transient aftereffect (Shadmehr and Mussa-Ivaldi 1994) of instability while the neural gains must readapt to the preferred configuration.

The adoption of a narrow stance in Parkinson's patients may be a compensatory strategy for the inflexibility in adapting to the biomechanical context of movement. Damage to the basal ganglia may impair the ability to modify postural muscle responses in response to changing postural configurations. Parkinson's subjects can maintain balance to postural pertur-

bation when standing but persist in activating leg muscle when subsequently seated (Horak et al. 1992). Similarly, the muscle activity evoked during standing balance perturbation responses is not modulated with stance width in Parkinson subjects (Dimitrova et al. 2004). These observations can be interpreted as an inability to adjust feedback gains associated with changing biomechanical constraints (Kim et al. 2009). Moreover, Parkinson subjects have characteristically stiff joint responses to perturbations (Horak et al. 2005). Stiffening may be the result of increased feedback gains, which our model suggests are less stable in wide stance. Thus patients with Parkinson's disease may select narrow stance to compensate for inflexible high gains, even though it may require greater muscle activity.

Predictions from our model should be interpreted as system-level phenomena, and finer grained analysis should "anchor" our "template" in a more detailed model (Full and Koditschek 1999). Our model does not speak to the physiological location of where sensorimotor feedback gain changes occur. However, others have shown that sensorimotor feedback pathways for balance control involve the brain stem (Deliagina et al. 2007; Macpherson et al. 1997) with cortical influences (Jacobs and Horak 2007). Intrinsic muscular or neural properties may also contribute to sensorimotor gain changes. For example, muscle torque production can be affected by moment arms (Young et al. 1992), muscle length (Huxley and Simmons 1971), or motoneuron gain (Hyngstrom et al. 2007) due to changes in configuration. Observations of muscle cocontraction in many neurological populations (Blood 2008; Dietz and Sinkjaer 2007) may be explained by expanding our model to include passive stiffness to quantify the contribution of cocontraction to postural balance stability. Predictions from this model may be used to guide future experimental research about motor variability, motor adaptation, energetic efficiency, and functional stability of standing balance.

Is Wide Stance More Stable?

Conventional wisdom suggests that wide stance is more stable, because one's intuition is to widen one's stance width when situations become more challenging. Our model demonstrates that the increase in stance width allows for larger center-of-mass excursions before a step is necessary. Furthermore, mechanical leverage at the hip is increased, allowing greater torque generation about the center of mass. A wider stance thus lessens the muscular effort required for balance control, improving the stability of the subject in the presence of a perturbation. However, our results demonstrate that this increase in functional stability is only possible when accompanied by appropriately scaled delayed neural feedback. The same mechanical effects that allow for reduced effort and larger responses to perturbations in wide stance also increase the inherent instability of the musculoskeletal system and limit the set of feasible stable feedback gains at wide stance. Thus an impaired nervous system may not be able to exploit the intuitive benefits of wide stance due to increased neural delay, improper context-dependent modulation, or increased sensorimotor noise. The perception of increased stability at wide stance is not simply due to changes in the biomechanics of the body but is predicated on the requisite flexibility of neural mechanisms controlling balance.

APPENDIX

Model

The four-bar linkage model was a single-degree of freedom system with the ankle angle, $q_A(t)$, selected as the generalized coordinate. The form of the equation of motion was separated into configuration-dependent inertial terms, $\mathbf{I}(q_A(t))$, centripetal and coriolis terms, $\mathbf{V}(q_A(t), \dot{q}_A(t))$, and gravitational terms, $\mathbf{G}(q_A(t))$.

$$\mathbf{I}(q_A(t))\ddot{q}_A(t) + \mathbf{V}(q_A(t), \dot{q}_A(t)) + \mathbf{G}(q_A(t)) = \mathbf{T}(q_A(t-\tau), \dot{q}_A(t-\tau)) + \mathbf{P}(q_A(t), t) \quad (1)$$

Generalized forces applied to the model were divided into joint torques, $\mathbf{T}(q_A(t-\tau), \dot{q}_A(t-\tau))$, and perturbations, $\mathbf{P}(q_A(t), t)$. The joint torque was dependent on delayed position and velocity values of the feedback signal, where the delay was signified by τ. The platform perturbation (*Eq. 2*) was applied as a generalized force with a configuration-dependent inertial term, C_P, and an acceleration profile, a. When experimentally measured accelerations were unavailable, the acceleration term consisted of two Gaussian pulses with opposite direction. The pulses were 40 ms wide (ρ), spaced 500 ms apart ($t_f - t_o$), and had amplitudes ranging from 0.1 to 0.5 g (A).

$$\mathbf{P}(q_A(t), t) = C_P(q_A(t))a(t) = C_P(q_A(t))A\left(e^{\frac{-(t-t_o)^2}{2\rho^2}} - e^{\frac{-(t-t_f)^2}{2\rho^2}}\right) \quad (2)$$

Linearization

For the stability analysis and sensitivity of parameters, the equations of motion with perturbation forces removed (*Eq. 1*) were linearized by taking the first-order Taylor series expansion about an equilibrium. The equilibrium angle of the ankle was defined with *Eq. 3*, where W is the hip width, S is the stance width, and L is the leg length:

$$q_{A_o} = \arccos\left(\frac{S - W}{2L}\right) \quad (3)$$

The equations of motion (*Eq. 4*) were then expressed as linear relations with respect to the generalized coordinate states and their delayed counterparts. Linearized inertial, $\mathbf{I}_e$, and gravitational, $\mathbf{G}_e$, terms were then expressed as constant coefficients for a specified configuration, and the coriolis terms, $\mathbf{V}$, vanished.

$$\mathbf{I}_e\ddot{q}_A(t) - \mathbf{G}_e q_A(t) = \mathbf{T}_i \quad (4)$$

The linearized inertia (*Eq. 7*) was represented as a single lumped value dependent on S and the subject-specific leg and trunk masses (m_{leg}, m_{trunk}), inertias (I_{leg}, I_{trunk}) and geometry [W, L, length from ankle to center of mass of leg (L_{COM}), and vertical distance from hip center to center of mass of torso (H_{COM})].

$$\delta = S - W \quad (5)$$

$$\eta = \frac{1}{2}\sqrt{4L^2 - \delta^2} \quad (6)$$

$$\mathbf{I}_e = 2(m_{leg}L_{COM}^2 + I_{leg}) + \frac{1}{W^2}\left[m_{trunk}(H_{COM}\delta - W\eta)^2 + I_{trunk}\delta^2\right] \quad (7)$$

Similarly, the linearized gravitational stiffness (*Eq. 8*) was dependent on subject-specific mass and geometry as well as stance width.

$$\mathbf{G}_e = \left[\frac{m_{trunk}(H_{COM}\delta^2)}{W^2} - \frac{(2L_{COM}m_{leg} + Lm_{trunk})(\delta\eta^2 - L^2S)}{LW\eta}\right]g \quad (8)$$

The linearized expression for the generalized torque (*Eq. 9*) was written in terms of the feedback law and a configuration-dependent term, ${}^{i}C$, that was specific to each type of feedback signal. For the following equations, the superscript i is a substitute for either hip or center-of-mass feedback signals.

$$\mathbf{T} = -{}^{i}C\frac{S}{W}[{}^{i}k_{\mathrm{p}}q_{\mathrm{A}}(t-\tau)+{}^{i}k_{\mathrm{v}}\dot{q}_{\mathrm{A}}(t-\tau)] \tag{9}$$

Two types of feedback signals were used. When hip angular position and velocity was used (*Eq. 10*), the configuration-dependent coefficient, ${}^{\mathrm{hip}}C$, was dependent only on the width of stance and distance between the hips.

$${}^{\mathrm{hip}}C = \frac{S}{W} \tag{10}$$

When the center-of-mass excursion was used as a feedback signal (*Eq. 11*), the expression for the configuration-dependent coefficient, ${}^{\mathrm{com}}C$, was more complex and was related to the height of the center of mass.

$${}^{\mathrm{com}}C = \frac{H_{COM}Lm_{trunk}\delta - W(Lm_{trunk}+2L_{COM}m_{leg})\eta}{LW(2m_{leg}+m_{trunk})} \tag{11}$$

Stability Boundaries

The closed-loop stability of the delayed feedback system was accomplished by analyzing the system about equilibrium (*Eq. 3*) and assuming exponential solutions to the differential equation. This resulted in the development of the following characteristic equation (*Eq. 12*):

$$\mathbf{I}_{\mathrm{e}}\lambda^2 - \mathbf{G}_{\mathrm{e}} + {}^{i}C\left(\frac{S}{W}\right)[k_{\mathrm{p}}e^{-\lambda\tau} + k\lambda e^{-\lambda\tau}] = 0 \tag{12}$$

The solutions to the characteristic equation become unstable when the real part transitions from negative to positive. Stability was then determined by finding solutions, values of $\lambda = r + j\omega$, to the characteristic equation that had strictly zero real part, $r = 0$. These solutions therefore were described as curves parameterized by the magnitude of the imaginary part, ω.

The left-hand boundary (*Eq. 13*) represented a lower limit on delayed position feedback gain, k_{p}, described by a fold bifurcation. The functional consequence of this limit corresponded to feedback stiffness, k_{p}, of the delayed position feedback gain being unable to counteract the destabilizing gravitational stiffness, $\mathbf{G}_{\mathrm{e}}$.

$$\mathrm{LHB} \equiv \begin{cases} {}^{i}k_{\mathrm{p}} = & \dfrac{1}{{}^{i}C}\dfrac{W}{S}\mathbf{G}_{\mathrm{e}} \\ {}^{i}k_{\mathrm{v}} = & \mathbb{R} \end{cases} \tag{13}$$

The right-hand boundary (*Eq. 14*) restricted both position and velocity feedback gains and was described by a Hopf bifurcation. This upper boundary was a consequence of the feedback delay and functionally represented an instability due to overcorrection.

$$\mathrm{RHB} \equiv \begin{cases} {}^{i}k_{p} = & \dfrac{1}{{}^{i}C}\left(\mathbf{I}_{\mathrm{e}}\omega^2 + \mathbf{G}_{\mathrm{e}}\right)\dfrac{W\cos(\tau\omega)}{S} \\ {}^{i}k_{p} = & \dfrac{1}{{}^{i}C}\left(\mathbf{I}_{\mathrm{e}}\omega^2 + \mathbf{G}_{\mathrm{e}}\right)\dfrac{W\sin(\tau\omega)}{\omega S} \end{cases} \tag{14}$$

Finally, an upper limit on the length of delay was found for which there were no feedback gain values that were stable (*Eq. 15*). This occurred when the right-hand boundary was reduced to a single point.

$$\tau_{\max} = \sqrt{\frac{2\mathbf{I}_{\mathrm{e}}}{\mathbf{G}_{\mathrm{e}}}} \tag{15}$$

Nondelayed Feedback

The four-bar linkage with delayed feedback may be extended to include nondelayed feedback terms. This modification includes additional torque components associated with passive stiffness, k, and damping, b, and the linearized equations of motion take on the form below.

$$\begin{aligned}\mathbf{I}_{\mathrm{e}}\ddot{q}_{\mathrm{A}}(t) - \mathbf{G}_{\mathrm{e}}q_{\mathrm{A}}(t) = &-{}^{i}C\frac{S}{W}[{}^{i}k_{\mathrm{p}}q_{\mathrm{A}}(t-\tau)+{}^{i}k_{\mathrm{v}}\dot{q}_{\mathrm{A}}(t-\tau)] \\ &- \frac{S^2}{W^2}\left[kq_{\mathrm{A}}(t) + b\dot{q}_{\mathrm{A}}(t)\right]\end{aligned} \tag{16}$$

The stability boundaries in terms of the delayed feedback gains are therefore found to have the following form:

$$\mathrm{LHB}^* \equiv \begin{cases} {}^{i}k_{\mathrm{p}} = & \dfrac{1}{{}^{i}C}\left(\dfrac{W}{S}\mathbf{G}_{\mathrm{e}} - \dfrac{S}{W}k\right) \\ {}^{i}k_{\mathrm{v}} = & \mathbb{R} \end{cases} \tag{17}$$

$$\mathrm{RHB}^* \equiv \begin{cases} {}^{i}k_{\mathrm{p}} = & \dfrac{1}{{}^{i}C}\left(\left(\mathbf{I}_{\mathrm{e}}\omega^2 + \mathbf{G}_{\mathrm{e}}\right)\dfrac{W\cos(\tau\omega)}{S} - \dfrac{S}{W}[k\cos(\tau\omega) - b\omega\sin(\tau\omega)]\right) \\ {}^{i}k_{\mathrm{v}} = & \dfrac{1}{{}^{i}C}\left(\left(\mathbf{I}_{\mathrm{e}}\omega^2 + \mathbf{G}_{\mathrm{e}}\right)\dfrac{W\sin(\tau\omega)}{\omega S} - \dfrac{1}{\omega}\dfrac{S}{W}[k\sin(\tau\omega) + b\omega\cos(\tau\omega)]\right) \end{cases} \tag{18}$$

ACKNOWLEDGMENTS

We thank K. van Antwerp for insightful comments.

GRANTS

This work was funded by National Institutes of Health Grants R01 NS053822 and HD04922 (to L. H. Ting).

DISCLOSURES

No conflicts of interest, financial or otherwise, are declared by the author(s).

REFERENCES

Allum JH, Carpenter MG, Honegger F, Adkin AL, Bloem BR. Age-dependent variations in the directional sensitivity of balance corrections and compensatory arm movements in man. *J Physiol* 542: 643–663, 2002.

Black HS. Stabilized feed-back amplifiers. *Trans Am Inst Electr Eng* 53: 114–120, 1934.

Blood AJ. New hypotheses about postural control support the notion that all dystonias are manifestations of excessive brain postural function. *Biosci Hypotheses* 1: 14–25, 2008.

Boling MC, Padua DA, Alexander Creighton R. Concentric and eccentric torque of the hip musculature in individuals with and without patellofemoral pain. *J Athl Train* 44: 7–13, 2009.

Bosco G, Poppele RE. Representation of multiple kinematic parameters of the cat hindlimb in spinocerebellar activity. *J Neurophysiol* 78: 1421–1432, 1997.

Bunderson NE, Burkholder TJ, Ting LH. Reduction of neuromuscular redundancy for postural force generation using an intrinsic stability criterion. *J Biomech* 41: 1537–1544, 2008.

Cuthbert SC, Goodheart GJ Jr. On the reliability and validity of manual muscle testing: a literature review. *Chiropr Osteopat* 15: 4, 2007.

Deliagina TG, Zelenin PV, Beloozerova IN, Orlovsky GN. Nervous mechanisms controlling body posture. *Physiol Behav* 92: 148–154, 2007.

Dietz V, Sinkjaer T. Spastic movement disorder: impaired reflex function and altered muscle mechanics. *Lancet Neurol* 6: 725–733, 2007.

Dimitrova D, Horak FB, Nutt JG. Postural muscle responses to multidirectional translations in patients with Parkinson's disease. *J Neurophysiol* 91: 489–501, 2004.
Engelborghs K, Luzyanina T, Roose D. Numerical bifurcation analysis of delay differential equations using DDE-BIFTOOL. *ACM Trans Math Software* 28: 1–21, 2002.
Franklin DW, Osu R, Burdet E, Kawato M, Milner TE. Adaptation to stable and unstable dynamics achieved by combined impedance control and inverse dynamics model. *J Neurophysiol* 90: 3270–3282, 2003.
Full RJ, Koditschek DE. Templates and anchors: neuromechanical hypotheses of legged locomotion on land. *J Exp Biol* 202: 3325–3332, 1999.
Goodworth AD, Peterka RJ. Influence of stance width on frontal plane postural dynamics and coordination in human balance control. *J Neurophysiol* 104: 1103–1118, 2010.
Henry SM, Fung J, Horak FB. Effect of stance width on multidirectional postural responses. *J Neurophysiol* 85: 559–570, 2001.
Hogan N. The mechanics of multi-joint posture and movement control. *Biol Cybern* 52: 315–331, 1985.
Horak FB, Dimitrova D, Nutt JG. Direction-specific postural instability in subjects with Parkinson's disease. *Exp Neurol* 193: 504–521, 2005.
Horak FB, Macpherson JM. Postural orientation and equilibrium. In: *Handbook of Physiology. Exercise: Regulation and Integration of Multiple Systems.* Bethesda, MD: Am Physiol Soc, 1996, sect. 12, p. 255–292.
Horak FB, Nutt JG, Nashner LM. Postural inflexibility in parkinsonian subjects. *J Neurol Sci* 111: 46–58, 1992.
Huxley AF, Simmons RM. Proposed mechanism of force generation in striated muscle. *Nature* 233: 533–538, 1971.
Hyngstrom AS, Johnson MD, Miller JF, Heckman CJ. Intrinsic electrical properties of spinal motoneurons vary with joint angle. *Nat Neurosci* 10: 363–369, 2007.
Jacobs JV, Horak FB. Cortical control of postural responses. *J Neural Transm* 114: 1339–1348, 2007.
Jang J, Hsiao KT, Hsiao-Wecksler ET. Balance (perceived and actual) and preferred stance width during pregnancy. *Clin Biomech (Bristol, Avon)* 23: 468–476, 2008.
Kaminski TW, Perrin DH, Gansneder BM. Eversion strength analysis of uninjured and functionally unstable ankles. *J Athl Train* 34: 239–245, 1999.
Kim S, Horak FB, Carlson-Kuhta P, Park S. Postural feedback scaling deficits in Parkinson's disease. *J Neurophysiol* 102: 2910–2920, 2009.
Konradsen L, Peura G, Beynnon B, Renström P. Ankle eversion torque response to sudden ankle inversion torque response in unbraced, braced, and pre-activated situations. *J Orthop Res* 23: 315–321, 2005.
Kuo AD. An optimal control model for analyzing human postural balance. *IEEE Trans Biomed Eng* 42: 87–101, 1995.
Kuo AD, Zajac FE. Human standing posture: multi-joint movement strategies based on biomechanical constraints. *Prog Brain Res* 97: 349–358, 1993.
Lockhart DB, Ting LH. Optimal sensorimotor transformations for balance. *Nat Neurosci* 10: 1329–1336, 2007.
Loram ID, Lakie M. Direct measurement of human ankle stiffness during quiet standing: the intrinsic mechanical stiffness is insufficient for stability. *J Physiol* 545: 1041–1053, 2002.
Macpherson JM, Fung J, Jacobs R. Postural orientation, equilibrium, and the spinal cord. *Adv Neurol* 72: 227–232, 1997.
Masani K, Vette AH, Kawashima N, Popovic MR. Neuromusculoskeletal torque-generation process has a large destabilizing effect on the control mechanism of quiet standing. *J Neurophysiol* 100: 1465–1475, 2008.
McGeer T. Passive dynamic walking. *Int J Rob Res* 9: 62–82, 1990.
McIlroy WE, Maki BE. Preferred placement of the feet during quiet stance: development of a standardized foot placement for balance testing. *Clin Biomech (Bristol, Avon)* 12: 66–70, 1997.
Mergner T. A neurological view on reactive human stance control. *Annu Rev Control* 34: 177–198, 2010.
Mergner T, Maurer C, Peterka RJ. A multisensory posture control model of human upright stance. *Prog Brain Res* 142: 189–201, 2003.
Milton JG, Cabrera JL, Ohira T. Unstable dynamical systems: delays, noise and control. *Europhys Lett* 83: 48001, 2008.
Norton RL. *Design of Machinery: An introduction to the Synthesis and Analysis of Mechanisms and Machines* (2nd ed.). New York: McGraw-Hill, 2001.
Pai YC, Maki BE, Iqbal K, McIlroy WE, Perry SD. Thresholds for step initiation induced by support-surface translation: a dynamic center-of-mass model provides much better prediction than a static model. *J Biomech* 33: 387–392, 2000.
Pai YC, Patton JL. Center of mass velocity-position predictions for balance control. *J Biomech* 30: 347–354, 1997.
Park S, Horak FB, Kuo AD. Postural feedback responses scale with biomechanical constraints in human standing. *Exp Brain Res* 154: 417–427, 2004.
Patton JL, Lee a W, Pai YC. Relative stability improves with experience in a dynamic standing task. *Exp Brain Res* 135: 117–126, 2000.
Peterka RJ. Comparison of human and humanoid robot control of upright stance. *J Physiol (Paris)* 103: 149–158, 2009.
Peterka RJ. Sensorimotor integration in human postural control. *J Neurophysiol* 88: 1097–1118, 2002.
Scrivens JE, Deweerth SP, Ting LH. A robotic device for understanding neuromechanical interactions during standing balance control. *Bioinspir Biomim* 3: 026002, 2008.
Seidel GK, Marchinda DM, Dijkers M, Soutas-Little RW. Hip joint center location from palpable bony landmarks—a cadaver study. *J Biomech* 28: 995–998, 1995.
Selen LP, Franklin DW, Wolpert DM. Impedance control reduces instability that arises from motor noise. *J Neurosci* 29: 12606–12616, 2009.
Shadmehr R, Mussa-Ivaldi FA. Adaptive representation of dynamics during learning of a motor task. *J Neurosci* 14: 3208–3224, 1994.
Sieber J, Krauskopf B. Complex balancing motions of an inverted pendulum subject to delayed feedback control. *Physica D* 197: 332–345, 2004.
Sponberg S, Full RJ. Neuromechanical response of musculo-skeletal structures in cockroaches during rapid running on rough terrain. *J Exp Biol* 211: 433–446, 2008.
Stepan G, Kollar L. Balancing with reflex delay. *Math Comput Model* 31: 199–205, 2000.
Swanenburg J, Bruin de ED, Uebelhart D, Mulder T. Falls prediction in elderly people: a 1-year prospective study. *Gait Posture* 31: 317–21, 2010.
Ting LH, van Antwerp KW, Scrivens JE, Mckay JL, Welch TD, Bingham JT, Deweerth SP. Neuromechanical tuning of nonlinear postural control dynamics. *Chaos* 19: 02611, 2009.
Torres-Oviedo G, Ting LH. Subject-specific muscle synergies in human balance control are consistent across different biomechanical contexts. *J Neurophysiol* 103: 3084–3098, 2010.
Trumbower RD, Krutky MA, Yang BS, Perreault EJ. Use of self-selected postures to regulate multi-joint stiffness during unconstrained tasks. *PloS One* 4: e5411, 2009.
Van Der Kooij H, Jacobs R, Koopman B, Der Helm van F. An adaptive model of sensory integration in a dynamic environment applied to human stance control. *Biol Cybern* 84: 103–115, 2001.
Weiss PL, Hunter IW, Kearney RE. Human ankle joint stiffness over the full range of muscle activation levels. *J Biomech* 21: 539–544, 1988.
Welch TDJ, Ting LH. A feedback model explains the differential scaling of human postural responses to perturbation acceleration and velocity. *J Neurophysiol* 101: 3294–3309, 2009.
Welch TDJ, Ting LH. A feedback model reproduces muscle activity during human postural responses to support-surface translations. *J Neurophysiol* 99: 1032–1038, 2008.
Winter DA. *Biomechanics and Motor Control of Human Movement* (3rd ed.). New York: Wiley, 2003.
Winter DA. Human balance and posture control during standing and walking. *Gait Posture* 3: 193–214, 1995.
Winter DA, Patla AE, Prince F, Ishac M, Gielo-Perczak K. Stiffness control of balance in quiet standing. *J Neurophysiol* 80: 1211–1221, 1998.
Woollacott M, Inglin B, Manchester D. Response preparation and posture control. Neuromuscular changes in the older adult. *Ann NY Acad Sci* 515: 42–53, 1988.
Ye H, Morton DW, Chiel HJ. Neuromechanics of coordination during swallowing in *Aplysia californica*. *J Neurosci* 26: 1470–1485, 2006.
Young RP, Scott SH, Loeb GE. An intrinsic mechanism to stabilize posture—joint-angle-dependent moment arms of the feline ankle muscles. *Neurosci Lett* 145: 137–140, 1992.